JOURNAL OF Materials CHEMISTRY

Magnetic and neutron diffraction studies on double perovskites A_2LnRuO_6 (A = Sr, Ba; Ln = Tm, Yb)

Yoshihiro Doi,*[a] Yukio Hinatsu,[a] Akio Nakamura,[b] Yoshinobu Ishii[b] and Yukio Morii[b]

[a]*Division of Chemistry, Graduate School of Science, Hokkaido University, Sapporo 060-0810, Japan. E-mail: doi@sci.hokudai.ac.jp; Fax: +81-11-706-4931; Tel: +81-11-706-2706*
[b]*Japan Atomic Energy Research Institute, Tokai-mura, Ibaraki, 319-1195, Japan*

Received 18th February 2003, Accepted 23rd April 2003
First published as an Advance Article on the web 16th May 2003

Magnetic properties of double perovskites A_2LnRuO_6 (A = Sr, Ba; Ln = Tm, Yb) have been reported. Powder neutron diffraction measurements have been performed at 10 K and higher temperatures ($\geqslant$100 K) to determine their crystal and magnetic structures. As a result of the Rietveld analysis of the diffraction profiles, it is found that they are monoclinic with space group $P2_1/n$ (A = Sr) or cubic with space group $Fm\bar{3}m$ (A = Ba). From the magnetic susceptibility and specific heat measurements, a magnetic transition at 36–48 K is observed in each compound. The neutron diffraction data collected at 10 K show that this magnetic transition is due to a long range antiferromagnetic ordering involving both Ru^{5+} and Ln^{3+} ions. Each of the magnetic moments of Ru^{5+} and Ln^{3+} orders in a type I arrangement.

Introduction

In recent years, the solid-state chemistry of mixed metal oxides containing platinum group metals has attracted a great deal of interest. In particular, ruthenium oxides with perovskite-related structures show a wide range of electronic properties.[1,2] We focused our attention on the structural chemistry and magnetic properties of the double perovskites A_2LnRuO_6 (A = Sr, Ba; Ln = Y, lanthanide elements) in which the Ln and Ru ions order alternately. These compounds contain a pentavalent ruthenium ion. Such a highly oxidized cation from the second transition series sometimes shows quite unusual magnetic properties. In addition, owing to the ordered arrangement between Ln and Ru ions, they are expected to show interesting magnetic behavior, reflecting the magnetic interaction between Ru and Ln ions.

Previously, we have investigated the magnetic properties of Sr_2LnRuO_6 (Ln = Eu–Lu) and have found that they show an antiferromagnetic transition at 30–46 K and a complicated temperature dependence of the magnetic susceptibilities below the transition temperatures.[3] The barium series of compounds Ba_2LnRuO_6 (Ln = Y, lanthanides) also show the antiferromagnetic transition and have higher Néel temperatures than those for the Sr series, T_N = 30–117 K.[4–8] The magnetic structures for some of the A_2LnRuO_6 compounds were determined by neutron diffraction measurements. For the A_2LnRuO_6 compounds containing nonmagnetic Ln^{3+} ions such as Y^{3+}, La^{3+}, and Lu^{3+}, only the Ru^{5+} ions order antiferromagnetically,[4,5,9] while in the case that the compounds contain magnetic Ln^{3+} ions (Ln^{3+} = Pr^{3+}, Nd^{3+}, Tb^{3+}, Ho^{3+}, and Er^{3+}), both the Ru^{5+} and Ln^{3+} ions order antiferromagnetically.[6–8,10–12] These results indicate that not only the magnetic interactions between Ru^{5+} ions but also those between Ru^{5+} and Ln^{3+} ions contribute to the magnetic ordering of the A_2LnRuO_6 compounds.

In order to deepen our understanding of the magnetic cooperative phenomenon due to the interactions between d (Ru^{5+}: $4d^3$) and f (Ln^{3+}: $4f^n$) electrons, it is necessary to prepare all the possible A_2LnRuO_6 with an ordered perovskite structure and to investigate their detailed magnetic properties and the magnetic structures. Although many studies on the magnetic properties and the magnetic structures of A_2LnRuO_6 have been reported,[3–12] those for A_2LnRuO_6 (A = Sr, Ba; Ln = Tm, Yb) have not been studied yet. We have successfully prepared these four compounds and performed their magnetic susceptibility, specific heat, and powder neutron diffraction measurements. In this paper, we will report the results and discuss the magnetic properties and magnetic structures for all the possible A_2LnRuO_6.

Experimental

Polycrystalline samples of A_2LnRuO_6 (A = Sr, Ba; Ln = Tm, Yb) were synthesized by a solid-state reaction. Powders of the alkaline earth carbonate ($SrCO_3$ or $BaCO_3$), the lanthanide sesquioxide (Tm_2O_3 or Yb_2O_3), and ruthenium dioxide (RuO_2) were used as starting materials (>99.9% purity). Stoichiometric amounts of them were mixed in an agate mortar. Each of the mixtures was pelletized and calcined in air at 1173 K for 12 h. The calcined materials were initially fired in air at 1473 K for 24–48 h, and were then fired at 1573 K for 60–84 h with several intermediate grindings and pelletings. The progress of the reactions was monitored by powder X-ray diffraction measurements. In addition, an isomorphous compound Ba_2LuNbO_6[13] with Ba_2LnRuO_6 was also prepared. This compound is a diamagnetic compound, and is needed to estimate the lattice contribution of the specific heat to the total specific heat of Ba_2LnRuO_6.

Powder neutron diffraction profiles were measured at 10 K and 100 K (or room temperature) using a high-resolution powder diffractometer (HRPD)[14] installed at the JRR3-M reactor (Japan Atomic Energy Research Institute), with a Si(533) monochromator (λ = 1.1624 Å) for Sr_2TmRuO_6 and with a Ge(331) monochromator (λ = 1.82255 Å) for other compounds. The collimators used were 6′-20′-6′ and were placed before and after the monochromator, and between the sample and each detector. The set of 64 detectors and collimators, which were placed every 2.5°, rotates around the sample. Crystal and magnetic structures were determined by the Rietveld technique, using the program RIETAN2000.[15]

The magnetic measurements were carried out using a SQUID magnetometer (Quantum Design, MPMS-5S). The temperature dependence of the magnetic susceptibilities was measured under both zero-field-cooled (ZFC) and field-cooled (FC) conditions in an applied field of 0.1 T over the temperature range of 2–300 K.

 DOI: 10.1039/b301935g

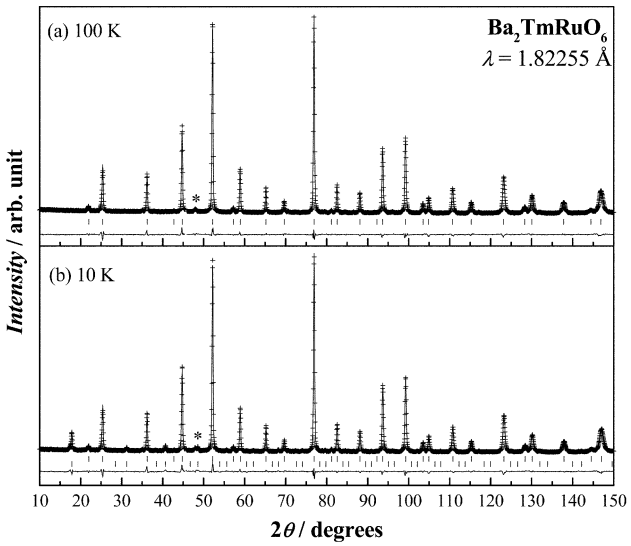

Fig. 1 Powder neutron diffraction profiles for Ba_2TmRuO_6 at 100 K (a) and at 10 K (b). In (a), the vertical marks show nuclear reflection positions, and in (b), upper and lower vertical marks show nuclear and magnetic reflection positions, respectively. The asterisk (*) denotes an impurity peak.

Specific heat measurements were performed using a relaxation technique with a commercial heat capacity measurement system (Quantum Design, PPMS model) in the temperature range of 1.8–300 K. The sintered sample in the form of a pellet was mounted on a thin alumina plate with grease for better thermal contact.

Results and discussion

Crystal structures

The neutron diffraction patterns for A_2LnRuO_6 (A = Sr, Ba; Ln = Tm, Yb) measured at 100 K or room temperature are shown in Figs. 1(a)–4(a). Small impurity phases of C-type Ln_2O_3 and/or 6H-$Ba_3LnRu_2O_9$[16] were detected. The Rietveld analysis containing both the main and impurity phases was carried out.

The neutron diffraction data for the Ba compounds (Ba_2TmRuO_6 and Ba_2YbRuO_6) were indexed in a cubic unit cell with space group $Fm\bar{3}m$ ($2a_p \times 2a_p \times 2a_p$), where a_p is the lattice parameter for the primitive perovskite ABO_3. On the other hand, the data for the Sr compounds (Sr_2TmRuO_6 and Sr_2YbRuO_6) show that they have a monoclinic unit cell with space group $P2_1/n$ ($\sqrt{2}a_p \times \sqrt{2}a_p \times 2a_p$), which corresponds to our previous result from X-ray diffraction measurements.[3] In both structures, the Ln^{3+} and Ru^{5+} ions structurally order over the six-coordinate B sites. Their typical crystal structures are illustrated in Fig. 5. The structural parameters, and some selected bond lengths and angles determined by the Rietveld analysis are listed in Tables 1–3. Neither the cation disorder between these two sites nor oxygen defect were found within the error of these analyses. The average Ru–O bond lengths are 1.957–1.971 Å, which agrees with those found in various ordered perovskites containing the Ru^{5+} ion, 1.953–1.963 Å[3–12] rather than with those in the perovskites $ARuO_3$ (A = Ca, Sr, Ba) containing the Ru^{4+} ion, 1.984–1.993 Å.[17–20]

The difference in the crystal structure between the Sr and Ba compounds can be explained by using the tolerance factor t. For ordered perovskites, $A_2B'B''O_6$, this factor is defined by

$$t = \frac{r_A + r_O}{\sqrt{2}\left(\frac{r_{B'} + r_{B''}}{2} + r_O\right)} \quad (1)$$

where r_A, $r_{B'}$, $r_{B''}$, and r_O are the ionic radii of the A, B′, B″, and

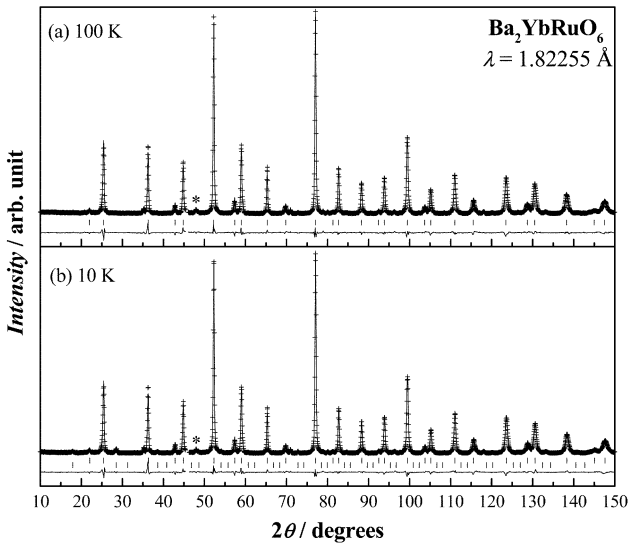

Fig. 2 Powder neutron diffraction profiles for Ba_2YbRuO_6 at 100 K (a) and at 10 K (b).

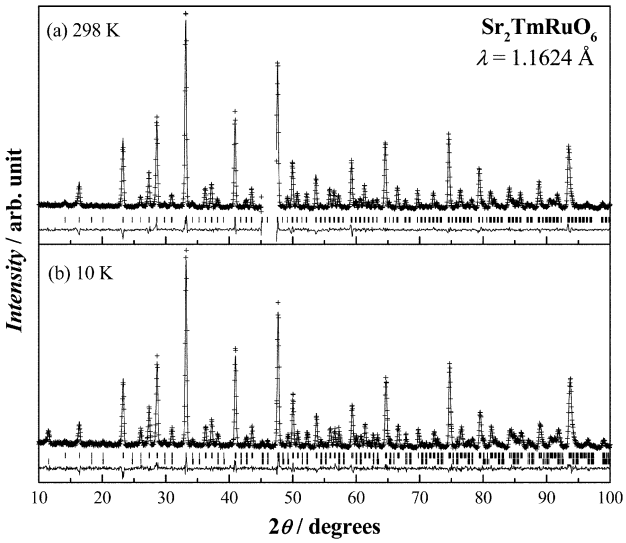

Fig. 3 Powder neutron diffraction profiles for Sr_2TmRuO_6 at room temperature (a) and at 10 K (b).

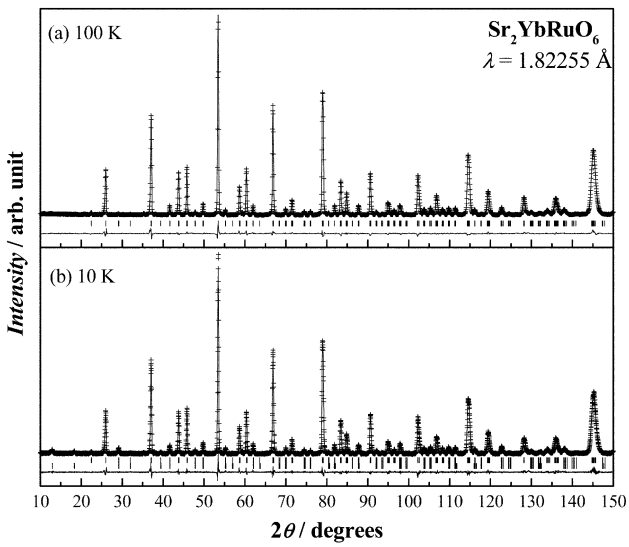

Fig. 4 Powder neutron diffraction profiles for Sr_2YbRuO_6 at 100 K (a) and at 10 K (b).

Table 1 Structural parameters for Ba_2LnRuO_6 (Ln = Tm, Yb) determined by neutron diffraction

Atom	Site	x	y	z	B/Å^2
Ba_2TmRuO_6 at 100 K					
Space group: $Fm\bar{3}m$, $z = 4$, $a = 8.2878(1)$ Å, $R_{wp} = 5.10\%$, $R_I = 2.05\%$, $R_F = 1.08\%$, $R_e = 4.35\%$					
Ba	8*c*	1/4	1/4	1/4	0.09(2)
Tm	4*b*	1/2	1/2	1/2	0.10(1)
Ru	4*a*	0	0	0	0.16(2)
O	24*e*	0.2366(1)	0	0	0.40(1)
Ba_2YbRuO_6 at 100 K					
Space group: $Fm\bar{3}m$, $z = 4$, $a = 8.2753(2)$ Å, $R_{wp} = 6.28\%$, $R_I = 1.56\%$, $R_F = 0.82\%$, $R_e = 4.40\%$					
Ba	8*c*	1/4	1/4	1/4	0.14(1)
Yb	4*b*	1/2	1/2	1/2	0.18(1)
Ru	4*a*	0	0	0	0.01(2)
O	24*e*	0.2382(1)	0	0	0.45(1)

O ions, respectively. For an ideal cubic perovskite structure, the value of t is equal to unity, whereas for structures distorted from the cubic symmetry, the value of t is <1. The calculated tolerance factors of A_2LnRuO_6 are 1.003 (for Ba_2TmRuO_6), 1.006 (for Ba_2YbRuO_6), 0.946 (for Sr_2TmRuO_6), and 0.949 (for Sr_2YbRuO_6). The tolerance factors for the Ba compounds are very close to one. On the other hand, those for the Sr compounds are <1. It is expected from eqn. (1) that the distortion of the crystal structure of A_2LnRuO_6 becomes significant with decreasing ionic size of the A ion and with increasing that of Ln ion. Actually, a series of Ba_2LnRuO_6 compounds adopts more distorted structures from the cubic symmetry with increasing ionic size of Ln ions, *i.e.*, they have the cubic (for Ln = Y, Eu, Er, Lu),[4,8,21] monoclinic (for Ln = Pr, Nd),[6,7] or triclinic (for Ln = La)[5] structures. The Sr_2LnRuO_6 compounds with a smaller A site ion (Sr^{2+}) than the Ba^{2+} ion adopt a monoclinic structure (for Ln = Y, Eu–Lu).[3] The result of the structural analysis in this study is in good agreement with this tendency.

The neutron diffraction profiles for A_2LnRuO_6 (A = Sr, Ba; Ln = Tm, Yb) at 10 K indicate that some additional reflection peaks exist which were not observed in the profiles at 100 K and room temperature. As will be described later, they are magnetic peaks due to an antiferromagnetic ordering of both Ln^{3+} and Ru^{5+}. The crystal and magnetic structures at 10 K have been determined by the Rietveld method. The crystal structure at 10 K has the same symmetry as that at higher temperatures, *i.e.*, A_2LnRuO_6 do not show any structural phase transitions down to 10 K.

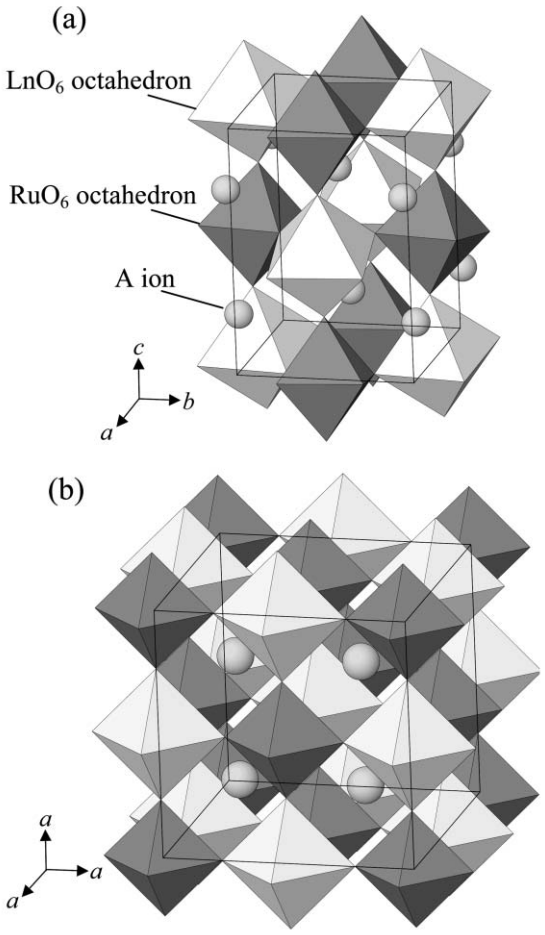

Fig. 5 Crystal structures of (a) Sr_2LnRuO_6 and (b) Ba_2LnRuO_6 (Ln = Tm, Yb).

Magnetic susceptibility

The temperature dependence of the magnetic susceptibilities for Ba_2TmRuO_6 and Ba_2YbRuO_6 are shown in Figs. 6(a) and 7(a). It is found that a magnetic anomaly has been observed at 42 and 48 K, respectively. No divergence has been observed between the ZFC and FC susceptibilities in the whole temperature range. The fitting of the Curie–Weiss law to the temperature dependence of magnetic susceptibilities at higher temperatures ($T > 200$ K) gives effective magnetic moments

Table 2 Structural parameters for Sr_2LnRuO_6 (Ln = Tm, Yb) determined by neutron diffraction

Atom	Site	x	y	z	B/Å^2
Sr_2TmRuO_6 at room temperature					
Space group: $P2_1/n$, $z = 2$, $a = 5.7553(4)$ Å, $b = 5.7542(4)$ Å, $c = 8.1332(8)$ Å, $\beta = 90.157(4)^\circ$, $R_{wp} = 7.43\%$, $R_I = 3.42\%$, $R_F = 1.31\%$, $R_e = 7.02\%$					
Ba	4*e*	0.0019(9)	0.0246(3)	0.2485(11)	0.74(3)
Tm	2*d*	1/2	0	0	0.47(4)
Ru	2*c*	1/2	0	1/2	0.20(4)
O(1)	4*e*	0.2658(9)	0.2955(9)	0.0326(7)	0.78(7)
O(2)	4*e*	0.2026(9)	−0.2304(10)	0.0322(7)	0.96(8)
O(3)	4*e*	−0.0634(9)	0.4890(7)	0.2383(6)	0.64(4)
Sr_2YbRuO_6 at 100 K					
Space group: $P2_1/n$, $z = 2$, $a = 5.7314(2)$ Å, $b = 5.7367(1)$ Å, $c = 8.1029(3)$ Å, $b = 90.182(1)^\circ$, $R_{wp} = 5.30\%$, $R_I = 1.65\%$, $R_F = 0.92\%$, $R_e = 4.30\%$					
Ba	4*e*	0.0055(5)	0.0258(3)	0.2480(5)	0.33(2)
Tm	2*d*	1/2	0	0	0.11(3)
Ru	2*c*	1/2	0	1/2	0.10(4)
O(1)	4*e*	0.2689(5)	0.2961(5)	0.0345(4)	0.43(6)
O(2)	4*e*	0.2018(5)	−0.2294(5)	0.0335(3)	0.37(5)
O(3)	4*e*	−0.0637(5)	0.4876(4)	0.2378(3)	0.31(5)

Table 3 Some selected bond lengths (Å) and angles (°) for A_2LnRuO_6 (A = Sr, Ba; Ln = Tm, Yb) at 100 K

	Sr_2TmRuO_6[a]	Sr_2YbRuO_6	Ba_2TmRuO_6	Ba_2YbRuO_6
Bond length				
Ln–O(1)	2.186(5)	2.173(3)	2.183(1)	2.167(1)
Ln–O(2)	2.181(5)	2.175(3)		
Ln–O(3)	2.160(5)	2.155(3)		
Average Ln–O	2.176(5)	2.168(3)		
Ru–O(1)	1.948(5)	1.954(3)	1.961(1)	1.971(1)
Ru–O(2)	1.958(6)	1.954(3)		
Ru–O(3)	1.974(5)	1.964(3)		
Average Ru–O	1.960(5)	1.957(3)		
Bond angle				
O(1)–Ln–O(2)	91.5(3)	91.3(1)	90	90
O(1)–Ln–O(3)	90.3(2)	90.0(1)		
O(2)–Ln–O(3)	90.3(2)	90.7(1)		
O(1)–Ru–O(2)	90.4(3)	90.6(1)	90	90
O(1)–Ru–O(3)	90.3(3)	90.8(1)		
O(2)–Ru–O(3)	90.3(2)	90.2(1)		

[a]The data at room temperature.

and Weiss constants. The respective values are 7.92(2) μ_B and −34(1) K for Ba_2TmRuO_6, and 4.20(6) μ_B and −181(6) K for Ba_2YbRuO_6. Since the theoretical free-ion magnetic moments of Ru^{5+}, Tm^{3+}, and Yb^{3+} are 3.87, 7.55, and 4.54 μ_B, respectively, the expected effective magnetic moments per formula unit are calculated to be 8.48 μ_B for Ba_2TmRuO_6 and 5.97 μ_B for Ba_2YbRuO_6. The values from the experiment are lower than the calculated values. This suggests that the magnetic ions in these compounds are affected by the crystal field to some extent.

The magnetic susceptibilities of Sr_2TmRuO_6 and Sr_2YbRuO_6 have been reported in our previous study.[3] They show an antiferromagnetic transition at 36 K and 44 K, respectively. Below these transition temperatures, divergences between the ZFC and FC susceptibilities are observed. This result indicates that Sr_2TmRuO_6 and Sr_2YbRuO_6 are not ideal antiferromagnets. We consider that this is due to the contribution of the weak ferromagnetic component to the magnetic properties.[3] For compounds with low crystal symmetry such as monoclinic symmetry, a Dzyaloshinsky–Moriya (D–M) interaction can exist between the ordered magnetic moments, and results in the ferromagnetic component to the magnetic susceptibility. On the other hand, Ba_2TmRuO_6 and Ba_2YbRuO_6 do not show divergence between the ZFC and FC susceptibilities. This fact is consistent with the result of the structural analysis in which they have a cubic structure.

Specific heat

Figs. 6(b) and 7(b) show the variation of the specific heat for Ba_2TmRuO_6 and Ba_2YbRuO_6 as a function of temperature. λ-Type anomalies have been observed at 42 K for Ba_2TmRuO_6 and at 48 K for Ba_2YbRuO_6, which correspond to the magnetic anomalies found in the magnetic susceptibility. The specific heat data for diamagnetic Ba_2LuNbO_6, which is isomorphous with Ba_2LnRuO_6, are also plotted in these figures. If these data are equal to the electronic and lattice contribution to the specific heat for Ba_2LnRuO_6, the magnetic specific heat (C_{mag}) for Ba_2LnRuO_6 is obtained by subtracting the specific heat of Ba_2LuNbO_6 from that of Ba_2LnRuO_6.

The temperature dependence of the magnetic specific heat and the magnetic entropy ($S_{mag} = \int(C_{mag}/T)dT$) for Ba_2YbRuO_6 is shown in Fig. 8. The magnetic entropy change

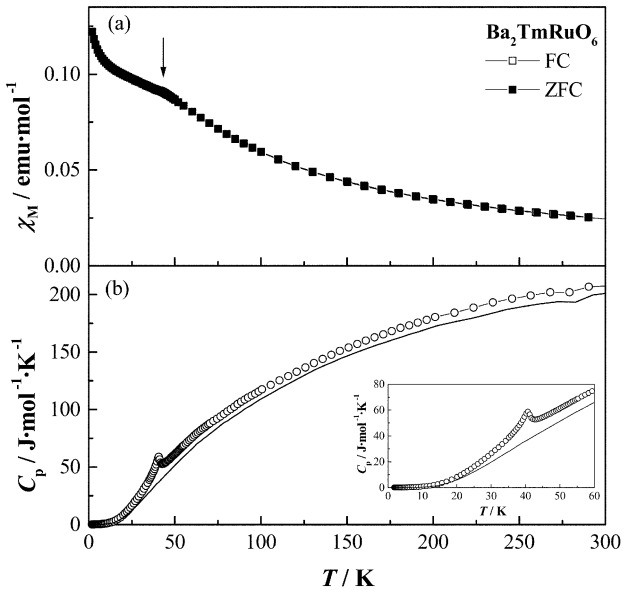

Fig. 6 Temperature dependence of (a) the magnetic susceptibilities and (b) specific heat for Ba_2TmRuO_6. In (b), a solid line shows the specific heat of Ba_2LuNbO_6. Inset shows the detailed specific heat at low temperatures.

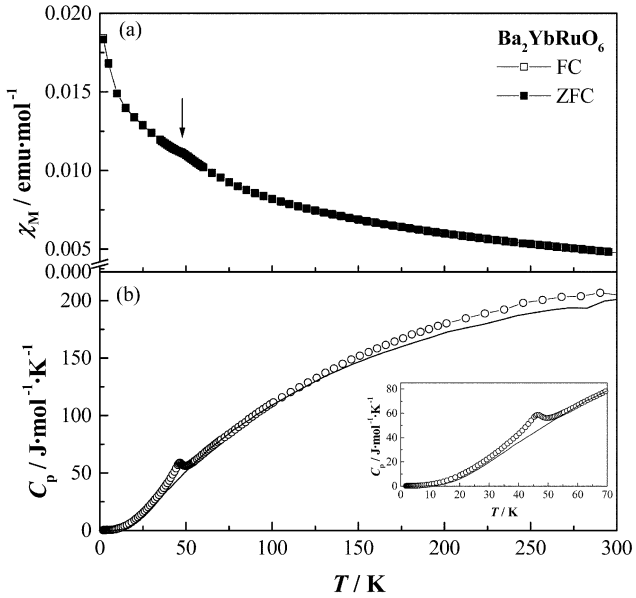

Fig. 7 Temperature dependence of (a) the magnetic susceptibilities and (b) specific heat for Ba_2YbRuO_6. In (b), a solid line shows the specific heat of Ba_2LuNbO_6. Inset shows the detailed specific heat at low temperatures.

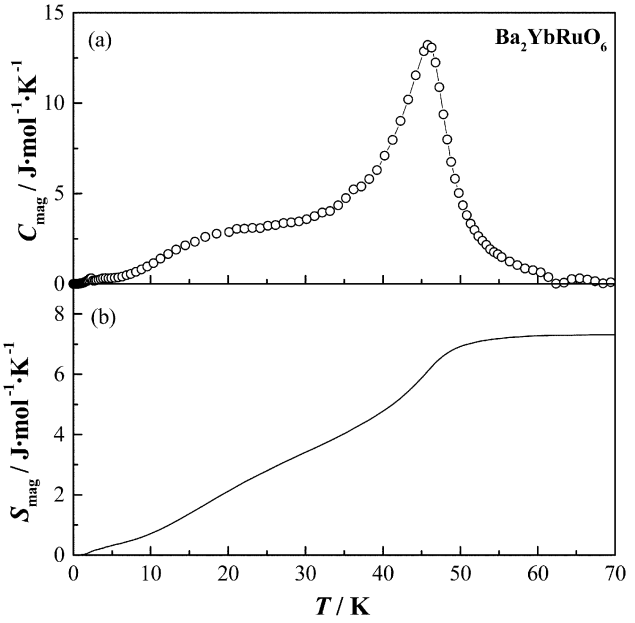

Fig. 8 Temperature dependence of (a) the magnetic specific heat and (b) magnetic entropy for Ba_2YbRuO_6.

associated with the magnetic transition observed at 48 K is estimated to be 7 J mol^{-1} K^{-1}. As will be described later, both Yb^{3+} and Ru^{5+} ions order antiferromagnetically in the magnetic structure of Ba_2YbRuO_6. Therefore, this value should contain a contribution from the magnetic ordering of both of these ions. Recently, the specific heat measurements for an isomorphous Ba_2YRuO_6, in which only the Ru^{5+} ions are magnetic, were reported, and the entropy change associated with the antiferromagnetic ordering of Ru^{5+} ions was estimated to be 3.9 J mol^{-1} K^{-1}.[8] If the magnetic entropy change for the Ru^{5+} ordering in Ba_2YbRuO_6 is the same as that in Ba_2YRuO_6, the rest of the magnetic entropy change of Ba_2YbRuO_6 ($\sim$3 J mol^{-1} K^{-1}) is due to the Yb^{3+} ordering. We believe that this value means the ground state of the Yb^{3+} ion to be doublet, although it is smaller than the expected value $R\ln W = R\ln 2 = 5.76$ J mol^{-1} K^{-1} (R: molar gas constant; W: number of states). The ground multiplet $^2F_{7/2}$ of Yb^{3+} is split into a doublet Γ_6 (ground state), a doublet Γ_7, and a quartet Γ_8 in the octahedral symmetry.[22] Therefore, the doublet ground state of Yb^{3+} ion found in the Ba_2YbRuO_6 is the Γ_6 state. This agrees with the result of the energy splitting of Yb^{3+} ions in the isomorphous compound Ba_2YbTaO_6.[23] The reason why the magnetic entropy changes estimated for Ru^{5+} and Yb^{3+} are smaller than $R\ln 2$ is not clear at present. This may be caused by an onset of the short-range magnetic ordering above T_N and/or an unsaturation of the ordered magnetic moment of Ln^{3+} ions.[10]

For Ba_2TmRuO_6, the magnetic entropy change associated with the magnetic transition observed at 42 K cannot be determined because of the poor fit of the specific heat data between Ba_2TmRuO_6 and Ba_2LuNbO_6 above T_N. The ground multiplet $^3H_6$ of Tm^{3+} is split into the Γ_1, Γ_2, Γ_3, Γ_4, and two Γ_5 states in an octahedral crystal field.[22] One reason why this estimation was unsuccessful in the Ba_2TmRuO_6 case may be that both the ground state (normally singlet Γ_1 or Γ_2) and low-lying excited states are populated around the magnetic transition temperature.

Magnetic structures

The neutron diffraction profiles for Ba_2LnRuO_6 (Ln = Tm, Yb) measured at 10 K are plotted in Figs. 1(b) and 2(b). The data collected at 10 K show a number of low angle peaks, which were not observed at 100 K and room temperature, indicating that these compounds exhibit a long-range magnetic ordering at low temperatures. The observed magnetic peaks can be indexed with the condition that each (h, k, l) reflection contains both an odd and even integer, and neither superlattice reflections nor magnetic satellite reflections are found. Therefore, the size of the magnetic unit cell is the same as that of the crystal unit cell at 100 K. A Rietveld analysis of the neutron diffraction data measured at 10 K was performed. In this analysis, we assumed that all the magnetic moments were collinear. The magnetic structures determined for Ba_2LnRuO_6 (Ln = Tm, Yb) are illustrated in Fig. 9. In these magnetic structures, each of the magnetic moments of Ln^{3+} and Ru^{5+} ions orders in a type I arrangement and the directions of the magnetic moments are parallel to the c axis. The difference between these magnetic structures is in the arrangement of the magnetic moments of Ln^{3+} and Ru^{5+} ions in the ab plane. In the case of Ba_2TmRuO_6, the moments of Ln^{3+} and Ru^{5+} are antiparallel with each other, while they are parallel for Ba_2YbRuO_6.

Figs. 3(b) and 4(b) show the neutron diffraction profiles for Sr_2LnRuO_6 (Ln = Tm, Yb) measured at 10 K. The observed magnetic peaks can be indexed with the condition that $[h + k + l]$ is an odd integer, and neither the superlattice reflections nor magnetic satellite reflections exist. The (001) magnetic reflection is negligible for Sr_2TmRuO_6 or very weak for Sr_2YbRuO_6; this fact indicates that the direction of the magnetic moments of Ln^{3+} and Ru^{5+} ions are parallel to the c axis for Sr_2TmRuO_6 or cant from the c axis to some extent for Sr_2YbRuO_6. Their magnetic structures have been determined by the Rietveld analysis, and are represented in Fig. 9.

The data concerning the magnetic structures of A_2LnRuO_6 (A = Sr, Ba; Ln = Y, lanthanides) compounds are

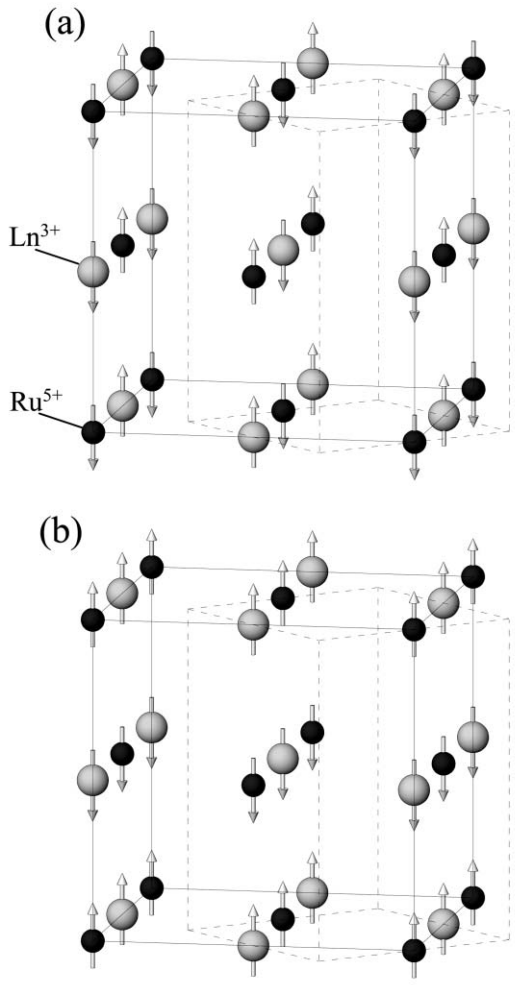

Fig. 9 Magnetic structures of (a) A_2TmRuO_6 and (b) A_2YbRuO_6 (A = Sr, Ba). The solid and dashed lines indicate the cubic and monoclinic unit cells, respectively.

Table 4 Magnetic structures of ordered perovskites A_2LnRuO_6 (A = Sr, Ba; Ln = Y, lanthanides) determined by neutron diffraction measurements

		Type of ordering			Ordered moments/μ_B				
Ln	A	Ru	Ln[a]	Angle/deg[b]	Ru	Ln	T_N/K	T_m/K[c]	Ref.
La	Ba	IIIa	—	($\perp a$)	1.96(10)	—	29.5	2	5
Pr	Ba	I	I_p	0	2.0(2)	2.2(1)	117	7	6
Nd	Ba	I	I_p	90	2.2(1)	2.3(1)	57	7	7
Tb	Sr	I	I_a	~20	2.99(11)	4.98(12)	41	10	12
Ho	Sr	I	I_a	0	2.74(9)	6.66(8)	36	10	11
	Ba	I	I_a	0	2.9	9.7	51	10	24
Er	Sr	I	I_a	90	1.74(6)	4.59(3)	42	4.2	10
	Ba	I	I_a	90	2.87(13)	4.43(8)	40	10	8
Tm	Sr	I	I_a	0	1.5(1)	1.4(1)	36	10	This work
	Ba	I	I_a	0	2.13(5)	1.91(3)	42	10	This work
Yb	Sr	I	I_p	23(2)	3.0(2)	0.92(8)	44	10	This work
	Ba	I	I_p	0	2.57(6)	1.00(3)	48	10	This work
Lu	Sr	I	—	[d]	2.10(8)	—	30	4.2	4
	Ba	I	—	[d]	2.06(6)	—	35	4.2	4
Y	Sr	I	—	[d]	1.85(10)	—	26	4.2	9
	Ba	I	—	[d]	2.11(6)	—	37[e]	4.2	4

[a]I_p: parallel arrangement of magnetic moments between Ln and Ru ions in the *ab* plane, I_a: antiparallel arrangement. [b]Direction of ordered magnetic moments against the *c* axis. [c]Temperature for measurements. [d]At least $\neq 0^\circ$ because a large (001) reflection was observed. [e]Ref. 8.

summarized in Table 4. The ordered magnetic moments of Ru^{5+} in this study are determined to be 1.5–3.0 μ_B. The theoretical value of the magnetic moment of Ru^{5+} ($4d^3$ electronic configuration) is 3.0 μ_B. The difference in the ordered moments may be attributed to the thermal fluctuations of the magnetic moments[10] and/or covalent effects. For the Tm^{3+} ion, the ground state is expected to be the nonmagnetic singlet state (Γ_1 or Γ_2) in an octahedral crystal field,[22] however, significant ordered moments (1.4(1) and 1.91(5) μ_B) were observed for Sr_2TmRuO_6 and Ba_2TmRuO_6, respectively. This fact indicates that the ground state of Tm^{3+} ions is not simple, and upper excited states such as Γ_4 and Γ_5 may contribute to the magnetic behavior of the Tm^{3+} ion. This result is similar to that of our previous study, *i.e.*, the ordered magnetic moment of the Pr^{3+} ion (2.2 μ_B) was observed in Ba_2PrRuO_6,[6] although the ground state of the Pr^{3+} ion is expected to be singlet (Γ_1) in an octahedral crystal field.[22] In this case, the observed ordered moments have been explained by the contribution from the first excited Γ_4 state.[6] The ordered moments of Yb^{3+} ions in A_2YbRuO_6 were determined to be ~1 μ_B. The ground state of Yb^{3+} is the Γ_6 state from the result of the specific heat measurements, as described earlier in this manuscript. The theoretical magnetic moment calculated from the Γ_6 state of Yb^{3+}[22] is $g_J\langle\Gamma_6|J_Z|\Gamma_6\rangle = 8/7 \times 7/6 = 1.33\ \mu_B$. This value is comparable with the ordered magnetic moments determined from the Rietveld analysis of the neutron diffraction measurements.

The magnetic structures of the A_2LnRuO_6 series are based on the type I ordering of Ru^{5+} and Ln^{3+} ions, except for the type IIIa ordering in Ba_2LaRuO_6 (see Fig. 9 and Table 4). For Ln = Y, La, Lu compounds, only the Ru^{5+} ions are magnetic. For such cases, the type of the magnetic ordering of the Ru^{5+} ions is determined by the relative strength of the two dominant magnetic interactions, one of which is the interaction between the nearest neighbor Ru^{5+} ion through the Ru–O–O–Ru pathway and the other one is the interaction between the next-nearest neighbor Ru^{5+} ion through the Ru–O–Ln–O–Ru pathway.[5] In the case that the Ln^{3+} ions are magnetic, their Néel temperatures are higher than those for the compounds containing the nonmagnetic Ln^{3+} ions, and the long range magnetic ordering of the Ln^{3+} ions is also observed by the analysis of the neutron diffraction data. These facts indicate that not only the magnetic interactions between Ru ions (Ru–O–O–Ru pathway) but also the interactions between Ru and Ln ions (Ru–O–Ln pathway) contribute to the magnetic ordering of the Ru^{5+} and Ln^{3+} ions. For each Ln ion, the magnetic structure of Ba_2LnRuO_6 is almost the same as that of Sr_2LnRuO_6 except for the difference in the magnitude of the ordered magnetic moments and for the canting of the magnetic moments from the *c* axis.

Acknowledgements

This work was supported by the Iketani Science and Technology Foundation.

References

1 Y. Maeno, H. Hashimoto, K. Yoshida, S. Nishizaki, T. Fujita, J. G. Bednorz and F. Lichtenberg, *Nature*, 1994, **372**, 532–534.
2 A. Callaghan, C. W. Moeller and R. Ward, *Inorg. Chem.*, 1966, **5**, 1572–1576.
3 Y. Doi and Y. Hinatsu, *J. Phys.: Condens. Matter*, 1999, **11**, 4813–4820.
4 P. D. Battle and C. W. Jones, *J. Solid State Chem.*, 1989, **78**, 108–116.
5 P. D. Battle, J. B. Goodenough and R. Price, *J. Solid State Chem.*, 1983, **46**, 234–244.
6 Y. Izumiyama, Y. Doi, M. Wakeshima, Y. Hinatsu, Y. Shimojo and Y. Morii, *J. Phys.: Condens. Matter*, 2001, **13**, 1303–1313.
7 Y. Izumiyama, Y. Doi, M. Wakeshima, Y. Hinatsu, K. Oikawa, Y. Shimojo and Y. Morii, *J. Mater. Chem.*, 2000, **10**, 2364–2367.
8 Y. Izumiyama, Y. Doi, M. Wakeshima, Y. Hinatsu, A. Nakamura and Y. Ishii, *J. Solid State Chem.*, 2002, **169**, 125–130.
9 P. D. Battle and W. J. Macklin, *J. Solid State Chem.*, 1984, **52**, 138–145.
10 P. D. Battle, C. W. Jones and F. Studer, *J. Solid State Chem.*, 1991, **90**, 302–312.
11 Y. Doi, Y. Hinatsu, K. Oikawa, Y. Shimojo and Y. Morii, *J. Mater. Chem.*, 2000, **10**, 797–800.
12 Y. Doi, Y. Hinatsu, K. Oikawa, Y. Shimojo and Y. Morii, *J. Mater. Chem.*, 2000, **10**, 1731–1737.
13 K. Henmi and Y. Hinatsu, *J. Solid State Chem.*, 1999, **148**, 353.
14 Y. Morii, *Nippon Kessho Gakkaishi*, 1992, **34**, 62–69.
15 F. Izumi and T. Ikeda, *Mater. Sci. Forum*, 2000, **321–324**, 198–203.
16 Y. Doi and Y. Hinatsu, *J. Mater. Chem.*, 2002, **12**, 1792–1795.
17 H. Kobayashi, M. Nagata, R. Kanno and Y. Kawamoto, *Mater. Res. Bull.*, 1994, **29**, 1271–1280.
18 W. Bensch, H. W. Schmalle and A. Reller, *Solid State Ionics*, 1990, **43**, 171–177.
19 C. W. Jones, P. D. Battle and P. Lightfoot, *Acta Crystallogr., Sect. C*, 1989, **45**, 365–367.
20 P. C. Donohue, L. Katz and R. Ward, *Inorg. Chem.*, 1965, **4**, 306–310.
21 T. C. Gibb and R. Greatrex, *J. Solid State Chem.*, 1980, **34**, 279–288.
22 K. R. Lea, M. J. M. Leask and W. P. Wolf, *J. Phys. Chem. Solids*, 1962, **23**, 1381–1405.
23 N. Taira and Y. Hinatsu, *J. Solid State Chem.*, 2000, **150**, 31–35.
24 Y. Hinatsu *et al.*, unpublished result.